# Contact Angles of Lennard-Jones Liquids and Droplets on Planar Surfaces

**T. Ingebrigtsen and S. Toxvaerd***

*Department of Chemistry, H. C. Ørsted Institute, DK-2100 Copenhagen Ø, Denmark*

*Received: November 16, 2006; In Final Form: April 18, 2007*

The contact angles of liquids and droplets of Lennard-Jones particles on a solid surface are determined by molecular dynamics simulations. The simulations show that the angles of contact are established within the first fluid layer. The droplets are not spherical segment-shaped. For an attractive surface corresponding to a small contact angle, the observed contact angles disagree with the corresponding angles obtained for macroscopic systems and using Young's equation and its extension for droplets with line tension.

## I. Introduction

The contact angle, $\theta$, between liquid and a (planar) solid surface is traditionally given by Young's equation[1] for $\theta$ and the surface tensions, $\gamma_{sv}$, between solid and vapor (sv), $\gamma_{lv}$, between liquid and vapor (lv) and $\gamma_{sl}$, and between solid and liquid (sl)

$$\gamma_{sv} = \gamma_{lv}\cos(\theta_\infty) + \gamma_{sl} \tag{1}$$

where $\theta_\infty$ is the contact angle of a macroscopic big liquid droplet at the surface. This equation ensures, according to Young, a force balance in the horizontal direction at a straight line on the solid surface where the three (infinitely large) planar surfaces, solid−liquid (sl), liquid−vapor (lv), and solid−vapor (sv), join. For a liquid in equilibrium with its corresponding vapor and in contact with a solid surface it must, however, have thermodynamic forces that balance. Strictly speaking, it is the relevant thermodynamic function for the system that is at minimum. For coexisting and not wetting liquid and vapor in equilibrium and on a planar surface, it is the total free energy that is minimum with respect to the area of contact between the solid and the liquid. In the molecular dynamics (MD) simulations of a droplet and its vapor, there is a constant number of particles, $N$, in a given volume, $V$, and temperature, $T$. The temperature is between the triple-point temperature and critical temperature and the ratio, $N/V$, is between the coexisting densities of liquid and vapor. For this MD system, it is the total Helmholtz free energy, $A(N,V,T,\mathcal{A})$, that is at minimum

$$\left(\frac{\partial A}{\partial \mathcal{A}}\right)_{N,V,T,\theta_\infty}|_{\mathcal{A}_{eq}} = 0 \tag{2}$$

for a macroscopic large droplet with a contact area, $\mathcal{A}_{eq} = \pi r_{dr}^2$ and contact angle, $\theta_\infty$, which expresses that the total Helmholtz free energy is minimum at equilibrium (eq). The macroscopic droplet has bulk liquid properties and a circular contact line with a radius, $r_{dr}$, so big that one can ignore the curvature effect along the circular line of contact. Young's equation is obtained by considering an infinitesimal change of the area of solid−liquid contact, $dA = 2\pi r_{dr}^2 dr_{dr}$ at constant $N,V,T$ and $\theta_\infty$, that is, the liquid front is parallel-shifted with $dr_{dr}$. This parallel shift of the liquid front changes the contact area of the bulk liquid with the solid by $d\mathcal{A}$, and the corresponding change in liquid−vapor contact area is $\cos(\theta_\infty)\, d\mathcal{A}$. Young's equation expresses that the three different thermodynamic works cancel.

$$dA = 0 = -\gamma_{sv}\, d\mathcal{A} + \gamma_{sl}\, d\mathcal{A} + \gamma_{lv}\cos(\theta_\infty)\, d\mathcal{A} \tag{3}$$

Young's equation gives a contact angle between macroscopic bulk phases. But because it is not possible to separate contributions to the free energy into the three subcontributions in an unambiguous way, when the range of the intermolecular forces exceeds, or is of the same order of magnitude as the "thickness" of the interfaces, the question is whether one can determine a contact angle with a resolution of a molecular diameter and whether the free-energy density near the surface scales in a way so that this contact angle can be identified as Young's angle of contact. In Section III, we show that one can determine a contact angle with nanoscale resolution and that this contact angle for small values near the wetting transition disagrees with Young's prediction.

In the present MD investigation of the contact angles of Lennard-Jones (LJ) droplets, the range of the intermolecular forces and energies is given by the weak dispersion energies, which in general are "short-ranged". These weak Van der Waals dispersion energies, which originate from the dynamic correlations of the valence electrons, are common for all atomic and molecular materials and decrease with the inverse power of six. But the total dispersion energy between a particle and the solid with a planar surface decreases much more slowly with the inverse power of three with respect to the distance to the solid surface. Thus, even for this L-J system, which must be the best real candidate to fulfill Young's equation on nanoscale resolution, the range of the force from the solid extends over many particle diameters ($\sigma$). In Figure 1, we have shown a typical density profile for a (wetting) liquid in equilibrium with its coexisting vapor. The oscillating density in the solid−liquid interface is a packing phenomenon caused by the strong repulsive forces. But a more detailed investigation shows (see Section III) that the impact of the attractive forces from the solid particles on the structure of the liquid extends over 5 to 10 $\sigma$. One can formulate the "problem" about the validity of Young's equation at molecular resolution as the following: only for a length scale essentially bigger than ∼5 nm is the range of the pair interactions so short-ranged that one can ignore this nanoscale contact problem in the L-J system. For ions and molecules with dipole moments, the range is much bigger. The

* Corresponding author. E-mail: tox@st.ki.ku.dk.

10.1021/jp0676235 CCC: $37.00 © 2007 American Chemical Society
Published on Web 05/25/2007

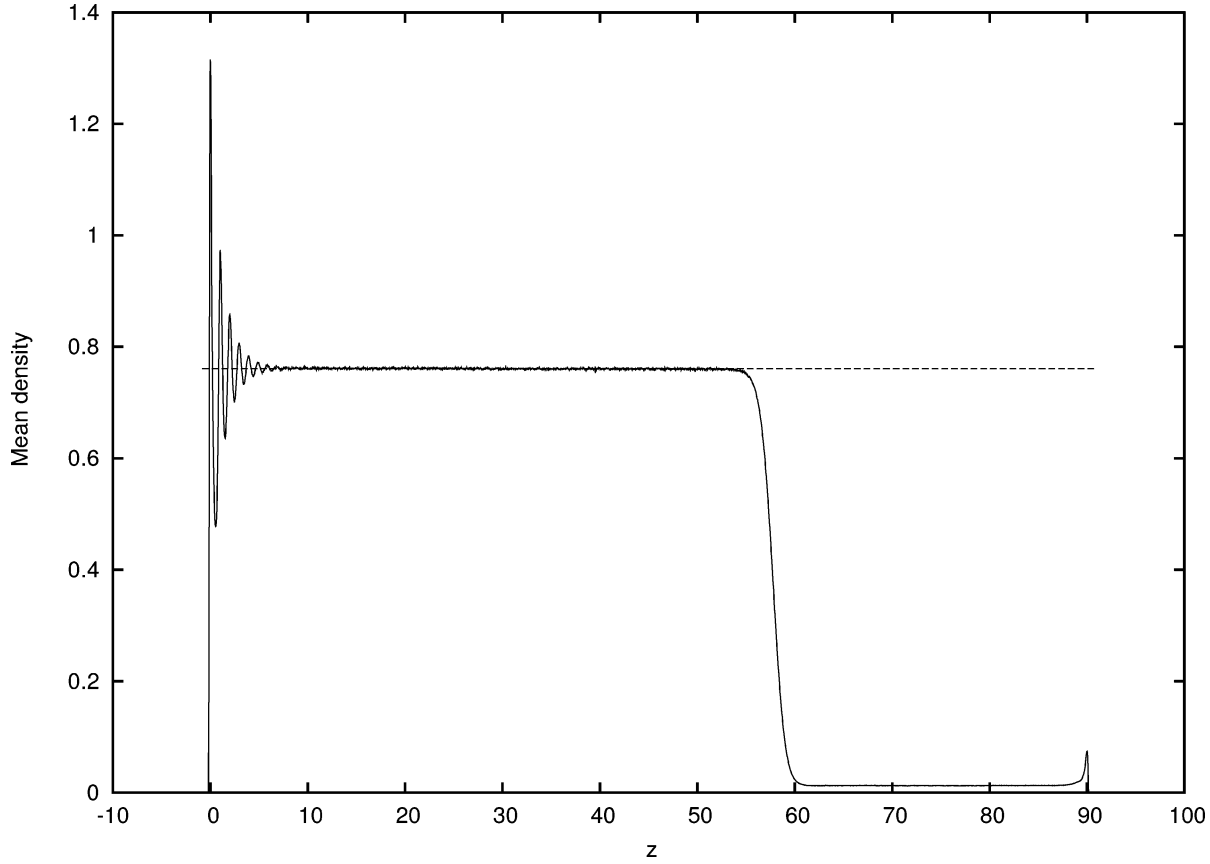


**Figure 1.** Density profile $\rho(z)$, in a system of 40 000 Lennard-Jones particles between semi-infinite solids with surfaces at $z = 0$ and $z = 90\ \sigma$ and a surface potential with $\rho_w \times f = 0.6$. $z$ is in units of $\sigma$, and density is in units of $\sigma^{-3}$. The mean densities are obtained for a simulation of 1 million time steps (~10 ns). The dotted line gives the density, $\rho_l = 0.7606$, in bulk liquid coexisting with the vapor with density $\rho_v = 0.0127$.

contact angle is, however, a real and observable quantity, and near wetting this nanoscale contact angle is different from the contact angle obtained from Young's equation.

The first to investigate the validity of Young's equation was G. Saville,[2] who also presented the arguments against the validity of the equation. His conclusion was that Young's equation is not valid. But the computer capability 30 years ago was not nearly sufficient to determine the angles and the values of the surface tensions of bulk phases in equilibrium. Later simulations[3,4] and investigations[5−7] have, however, ignored his objections and have instead collected the deviations from Young's equation for droplets in a free-energy contribution, $\tau$, due to the line tension[8]

$$\cos(\theta) = \cos(\theta_\infty) - \frac{\tau}{\gamma_{lv} r_{dr}} \tag{4}$$

where $\cos(\theta_\infty)$ is the contact angle of an infinitely large droplet and where the circular contact line of a spherical droplet has a radius, $r_{dr}$. The objection against this continuum formulation is the same as the objection against Young's equation. Furthermore, there are other effects that are ignored in this equation such as the curvature dependence of $\gamma_{lv}$,[9] and its finite-size dependence (reduced capillary wave-spectrum). A priori, one should expect a positive line tension; but eq 4 just serves as a correction to Young's equation, where all effects and shortcomings are collected in the value of $\tau$. This fact explains that one often obtains a negative line tension when using eq 4.

The MD systems and the computational details are given in the next section (II), and the results are presented in Section III. The discussion and conclusion are given in Section IV.

## II. Molecular Dynamics System

**A. Determination of the Surface Tensions.** The MD systems for the determination of surface tension of planar interfaces consist of $N = 40\,000$ L-J particles (truncated and shifted at $r = 2.5\ \sigma$) within a volume $V = l^2 \times l_z$ and with periodic boundaries in the $x$ and $y$ directions. In the $z$ direction, the $N$ particles are confined between $z = 0$ and $z = l_z$. The systems are calibrated at the temperature $T = 0.75$.[10] At this temperature, the vapor density is $\rho_v = 0.0127$ and the density, $\rho_l$, of coexisting bulk liquid is $\rho_l = 0.7606$ (Figure 1). The simplest L-J solid with a planar surface, and most commonly used solid in MD simulations, is the so-called "9−3" L-J potential, which is obtained by integrating the potential energy between a L-J particle at the $z$ position and a semi-infinite continuum below the plane $z = 0$, of uniformly distributed L-J particles with the density, $\rho_w$. The potential energy between a particle and this semi-infinite continuum is

$$u_{9-3}(z) = \frac{2\pi\rho_w\sigma^3}{3}\epsilon\left[\frac{2}{15}\left(\frac{z+\Delta}{\sigma}\right)^{-9} - \left(\frac{z+\Delta}{\sigma}\right)^{-3}\right] \tag{5}$$

where the lower part of the two semi-infinite planes is placed at $z = -\Delta = -(2/5)^{1/6}\sigma$ and the upper part correspondingly at $z = l_z + \Delta$, by which the force on a particle is zero at $z = 0$ and $z = l_z$. Furthermore, one can treat the attraction and the repulsion separately by varying the strength of the attractions, for example, as

$$u_{att}(z) = f \times u_{9-3}(z) \tag{6}$$

for $z \geq 0$. In the present investigation, the repulsive walls are the same for all of the simulations (with $\rho_w = 0.6$), which ensures a constant total volume, $V$. The contact angles and surface tensions are determined for three values of the strength of the attraction, $f \times \rho_w = 1$, $f \times \rho_w = 0.6$, and $f \times \rho_w = 0.3$, which results in contact angles $\theta \approx 40°$, $\theta \approx 95°$, and $\theta \approx 130°$, respectively.

The $u_{9-3}(z)$ potential has been used in models for contact angles,[2] wetting and pre-wetting at solid surfaces[11,12] and heterogeneous nucleation.[13] The potential parameters introduced by Ebner and Sam[11] for pre-wetting of Ar at a solid $CO_2$ surface correspond to an attractive strength of $\rho_w \times f = 1.67$, so the present walls can be characterized as rather soft surfaces with weak attractions and without pre-wetting.

The external $u_{9-3}$ potentials contribute to the sl and sv surface tensions, which are obtained as[14,15]

$$\gamma = \frac{1}{\mathcal{A}} \sum_{i}^{N} \sum_{j>i}^{N} \left\langle \frac{x_{ij}^2 + y_{ij}^2}{2} - z_{ij}^2 \frac{\mathrm{d}u(r_{ij})}{r_{ij}} \frac{\mathrm{d}r_{ij}}{\mathrm{d}z_i} - z_i \frac{\mathrm{d}u_{9-3}(z_i)}{\mathrm{d}z_i} \right\rangle \quad (7)$$

In MD systems, the pair potentials are usually truncated (and shifted) at a certain distance, $r_c$; for L-J particles usually at $r_c = 2.5\,\sigma$. The contributions to the tensions from longer-ranged interactions are, however, not negligible. If one wants to compare the calculated tensions with, for example, the tensions for a noble gas system, then one needs, however, not only to include the contributions from the longer-ranged interactions, for example, as a mean field correction,[16] but also to account for three-body interactions.[17] But when the contact angles of liquids of the truncated L-J particles are compared with the corresponding angles obtained from Young's equation one shall, however, not include the contributions for $r_c > 2.5\sigma$ to the surface tensions.

The present investigation indicates that, in order to obtain the value of the surface tensions for systems of 40 000 L-J particles (with $r_c = 2.5\,\sigma$) with an accuracy of the order of a few percent, one shall run the simulation for 1 million to 10 million time steps, corresponding to 10−100 ns. It is still a very big computer simulation using today's computers, and all of these facts are probably the reason that the calculated values of the surface tension reported in the literature are rather scattered even for the simple Lennard-Jones system. But these long simulations are needed to determine surface tensions, in order to determine whether the total free energy scales in a way so that Young's equation is also valid for the angle at the contact and with molecular-size resolution.

**B. Determination of the Contact Angles.** The contour of the liquids and droplets and Young's angles are determined in two steps: During the MD simulations, the particles in a droplet at a given time are obtained in the usual way using the "Stillinger criterion".[18] According to this criterion, a particle belongs to a given cluster if it is within a given (short) distance, $r_{cl}$, from at least one of the other particles in the cluster. The value of $r_{cl}$ is typically set to 1.5. The identification of the particles in the droplet at a given time also gives the time evolution of the position, $X(t)$, $Y(t)$, $Z(t)$, of the center of mass of the liquid droplet, and the number, $N_{cl}(t)$, of particles in the droplet gives a sensitive measure for when the droplet is in equilibrium. It is determined as the time from which there no longer is a drift $N_{cl}(t)$. Figure 2 shows such a time evolution of number of particles in a droplet of ∼70 000 particles. The position of *all* of the $N$ particles in the droplet

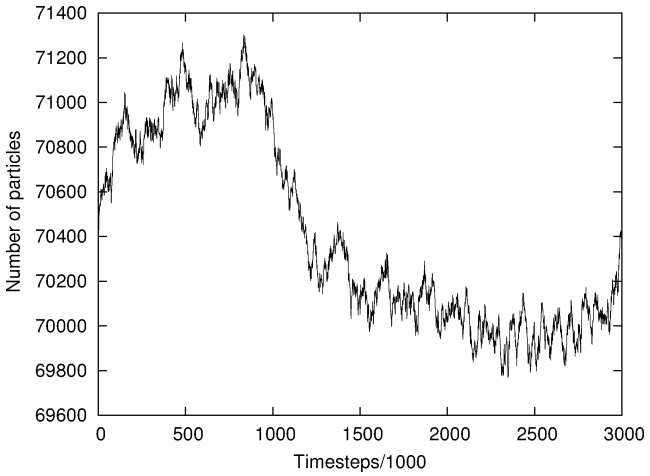


**Figure 2.** Number of particles in a large droplet during 3 million time steps. The instantaneous population is determined every 1000 time steps. The last 1 million steps (∼10 ns) are used to determine Young's contact angle.

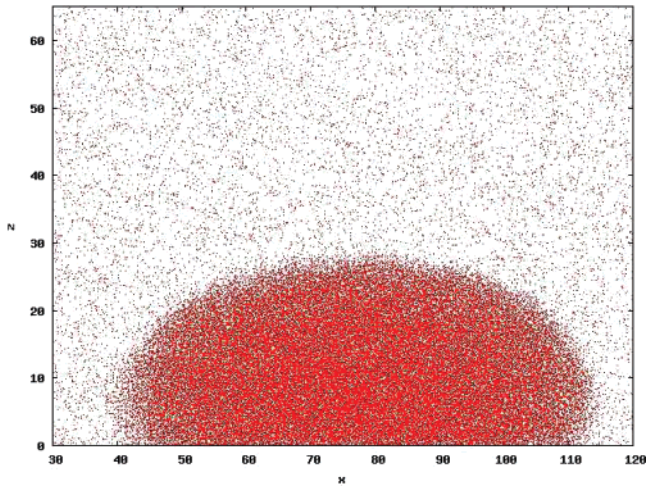


**Figure 3.** Side view of the droplet of ∼70 000 particles and for a reduced solid attraction given by $f \times \rho_w = 0.3$.

and the vapor at time $t$ is recorded in a coordinate system with center, $X(t)$, $Y(t)$, 0, at the $X(t)$, $Y(t)$ center-of-mass coordinates of the droplet, and these positions are used to evaluate the mean density in the droplet and the contact angle. Figure 3 shows a side view of the positions of all of the particles. To get an accurate determination of the density in the droplets, we have, however, averaged over many more time-sets, $\mathcal{N} = 1000$ sets of positions obtained from 1million time steps by recording the relative positions every thousand time steps.

The $\mathcal{N}$ sets of relative positions are used to determine the local density, $\rho(\mathbf{r})$, by dividing the volume, $V$, into parallel sheets with a spacing, $\Delta z$. The rotational symmetry in the local sheets is used to obtain the mean density, $\rho_{\alpha,\beta}$, in cylindrical volume elements centered at $X(t)$, $Y(t)$, $z_\beta$, as the mean number of particles in the subvolume $\Delta\tau_{\alpha,\beta} = \pi \times (r_{\alpha+1,\beta}^2 - r_{\alpha,\beta}^2) \times \Delta z$ of the $\alpha$th cylindrical ring and the $\beta$th sheet. By this evaluation, we do not a priori assume a spherical shape of the droplets. (The density profiles for liquids are obtained in a similar way.)

An example of the density variation across the surface of a droplet is shown in Figure 4. The figure shows the density profile in the first sheet in the droplet shown in Figure 3.

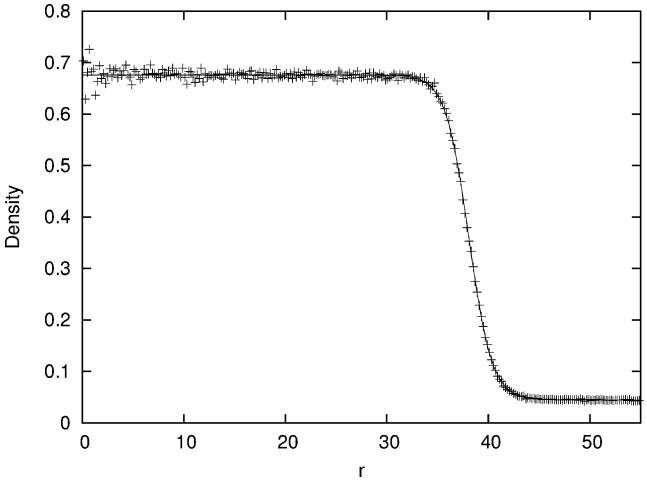


**Figure 4.** Density, $\rho(r)$, in the first sheet in the droplet shown in Figure 3, as a function of the distance, $r$, from the center of the droplet. The fitted tanh function is shown using a full line.

To determine the location of the surface of the droplets and the contact angle, we use the empirical tanh function[19]

$$\rho(r) = \frac{1}{2}(\rho_\beta(\mathrm{dr}) + \rho_\beta(\mathrm{g})) - \frac{1}{2}(\rho_\beta(\mathrm{dr}) - \rho_\beta(\mathrm{g}))\tanh\left(\frac{2(r - r_\beta)}{d_\beta}\right) \quad (8)$$

where $\rho_\beta$(dr) is the density inside the droplet in sheet no. $\beta$, and $\rho_\beta$(g) is the gas density outside. The thickness of the interface is given by $d_\beta$. The location of the surface at $z_\beta$ is given by $r_\beta$ and is used to obtain the contact angle. The fitting parameters $\rho_\beta$(dr), $\rho_\beta$(g), $d_\beta$, and $r_\beta$ gave excellent fits as can be seen in Figure 4.

The contact angle can be obtained as the limit value of the ratio between the spacing, $\Delta z$, of the sheets and the difference in the locations of Gibbs dividing surfaces, $r_2 - r_1$, in the two first sheets in a droplet

$$\theta = \lim_{\Delta z \to 0} tan^{-1}\left(\frac{\Delta z}{r_2 - r_1}\right) \quad (9)$$

A "resolution" value of $\Delta z \ll 1\sigma$, however, makes no sense. The oscillating densities near the wall are not a phenomenon connected with the contact angle but are instead a packing phenomenon present in all solid−liquid interfaces[15] including droplets. A priori, one shall expect a monotonic variation of the slope of the tangent to the surface of the droplet with respect to the distance to the surface. The demand for monotonic behavior of $\theta$ with respect to the spacing of the sheet provides a criterion for how small a value of $\Delta z$ one can use. We obtained monotonic behavior for the location of the dividing surface and thereby a monotonic behavior of the slope of the tangent to the surface of the droplet for a spacing larger than $\Delta z_{\min} \approx 0.7\sigma$. A criterion for the accuracy of the values for the contact angle is obtained by calculating the location of the dividing surface for a spacing $\Delta z = \Delta z_{\min} + 0.2\sigma$. We obtained differences in the values of $\leq 2°$.

The contact angle for a liquid front without line tension is determined as the angle at the edge of the meniscus of a bulk liquid in contact with a wall, in a similar way as for the droplets. The MD system was extended to $N = 160\,000$ L-J particles within a box with solid walls also at $(x,y)$ planes at $x = 0$ and $x = l_x = 60\sigma$. The length of the contact line in the $y$ direction was $60\sigma$. Figure 5 shows a side view of the big system.

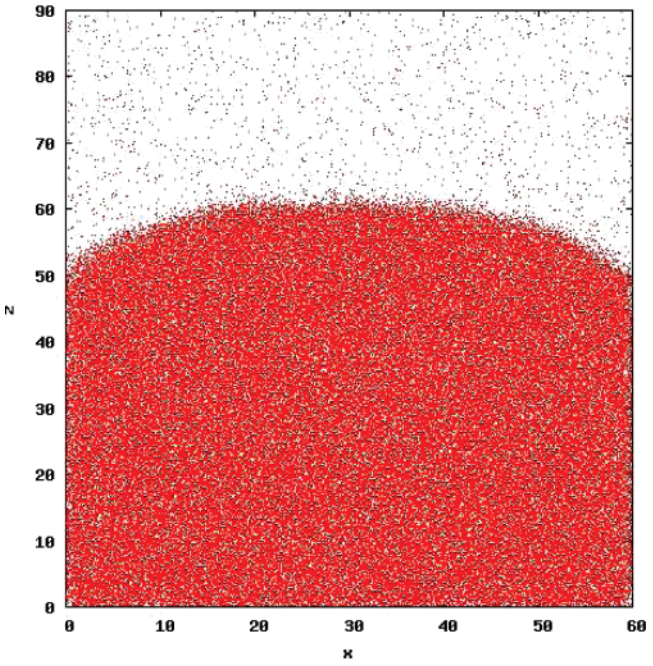


**Figure 5.** View in the $y$ direction of a set of positions of 160 000 L-J particles in a box with solid walls also at $(x,y)$ planes at $x = 0$ and $x = l_x$ ($= 60\sigma$) and with $f \times \rho_w = 0.3$ at all (three) solid planes. The contact angle, $\theta_\infty$, is obtained in a similar way as $\theta$ for the droplets.

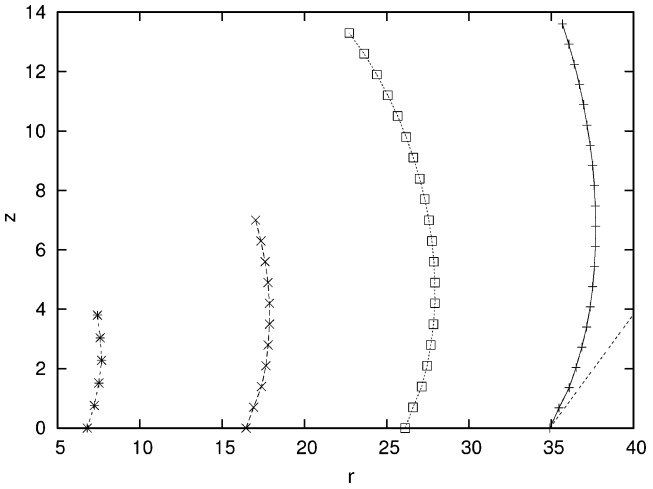


**Figure 6.** Droplet profiles for droplets on the weak attractive surface (Table 2). The surfaces (right part of) are located at $(r,z)$, where $r$ is the distance from the center of mass of the droplet. The dotted straight line shows the contact angle, $\theta_\infty$(Young) = 143, obtained from Young's equation.

## III. Results

The surface tensions of systems of $N = 40\,000$ L-J particles for $T = 0.75$ and for the three different strengths of surface attraction: $f \times \rho_w = 1$, $f \times \rho_w = 0.6$, and $f \times \rho_w = 0.3$, respectively, were obtained in two to three steps. First, we determined the densities of coexisting liquid and vapor by a MD system with a planar layer of liquid and periodical boundaries in all directions (i.e., no solid planes). The coexisting liquid and vapor densities as well as the value of the surface tension, $\gamma_{lg}$, agreed with the corresponding values obtained for the system shown in Figure 1. This means that the solid−liquid−gas system (Figure 1) is large enough to ensure uncorrelated solid−liquid and liquid−vapor interfaces. This was also confirmed by simulating a liquid in between two semi-infinite solids and adjusting the bulk liquid density (by scaling in the $z$

**TABLE 1: Surface Tensions, Young's Contact Angles, $\theta_\infty$(Young) and the Contact Angles, $\theta_\infty$, at Liquid Meniscus and for Different Strengths of Attraction $f \times \rho_w$ of the Solid[a]**

| $f \times \rho_w$ | $\gamma_{sl}$ | $\gamma_{lv}$ | $\gamma_{sv}$ | $\theta_\infty$(Young) | $\theta_\infty$ |
|---|---|---|---|---|---|
| 0.3 | $0.375 \pm 0.006$ | $0.489 \pm 0.003$ | $-0.014 \pm 0.001$ | $143° \pm 3°$ | $137° \pm 1°$ |
| 0.6 | $0.028 \pm 0.006$ | " | $-0.014 \pm 0.001$ | $95° \pm 3°$ | $99° \pm 1°$ |
| 1.0 | $-0.548 \pm 0.006$ | " | $-0.062 \pm 0.001$ | $6° \pm 3°$ | $39° \pm 1°$ |

[a] The values of the surface tensions are given in units of $\epsilon\sigma^{-2}$ and are for a truncated L-J system with $r_c = 2.5\sigma$

**TABLE 2: Droplet Sizes and Contact Angles for $f \times \rho_w = 0.3$ (Weak Attraction)**

| $\langle N \rangle$ | $r_1/\sigma$ | $\theta$/deg |
|---|---|---|
| 1070 | 6.27 | 117 |
| 8988 | 16.45 | 123 |
| 27 488 | 26.12 | 124 |
| 70 894 | 34.92 | 129 |
| 160 000 | $\infty$ | 137 |
| $\infty$(Young) | $\infty$ | 143 |

**TABLE 3: Droplet Sizes and Contact Angles for $f \times \rho_w = 0.6$ (Medium Attraction)**

| $\langle N \rangle$ | $r_1/\sigma$ | $\theta$/deg |
|---|---|---|
| 1750 | 9.46 | 83 |
| 9022 | 20.17 | 88 |
| 27 036 | 30.63 | 91 |
| 70 262 | 38.08 | 97 |
| 160 000 | $\infty$ | 99 |
| $\infty$(Young) | $\infty$ | 95 |

**TABLE 4: Droplet Sizes and Contact Angles for $f \times \rho_w = 1.0$ (Strong Attraction)**

| $\langle N \rangle$ | $r_1/\sigma$ | $\theta$/deg |
|---|---|---|
| 1125 | 12.16 | 37 |
| 9386 | 30.15 | 36 |
| 21 899 | 45.96 | 37 |
| 64 369 | 45.02 | 44 |
| 160 000 | $\infty$ | 39 |
| $\infty$(Young) | $\infty$ | 6 |

direction) to the value for the liquid density of coexisting liquid and vapor. The obtained value for the solid−liquid surface tension, $\gamma_{sl}$, also agreed with the corresponding value obtained from the solid−liquid−gas system (Figure 1). For significantly smaller systems this is, however, not the case, and the results demonstrate on one hand that the system is big enough to ensure that the interfaces in Figure 1 are not correlated and, on the other hand, that only a liquid−vapor interface a decade of molecular diameters away from the solid is uncorrelated with the solid−liquid interface. This indicates that the effect of the attractive forces from solid particles on the structure of the liquid−vapor interface, and thereby the surface tension, is over many molecular diameters. The values determined from $10^7$ time steps are given in Table 1 together with the values of Young's contact angles, $\theta_\infty$(Young), obtained from the surface tensions and using Young's equation. The three strengths of attraction predict contact angles from near wetting to an angle of 143° for the surface with the weak attraction.

According to Young's equation, the curvature of the Helmholtz free energy at the minimum is proportional to $\gamma_{lv} \sin\theta$ with the consequence that the shape of the droplets fluctuates for small contact angles near wetting and for large contact angles near de-wetting ($\theta \approx 180°$) of the droplet. The simulations demonstrated this fact. For the strong attraction with a small contact angle, the shape of the droplets was difficult to determine even after equilibration of many million time steps. To estimate the accuracy of the results (Tables 1−4), we have therefore equilibrated these droplets starting with different droplet shapes and obtained contact angles with an accuracy of ~1°.

The profiles were determined for the liquids and different droplets and for the three different strengths of surface attraction. The results are collected in Tables 1-4. The three different contact angles, $\theta_\infty$, for the meniscus of a liquid at a wall are in Table 1 compared with the corresponding contact angles, $\theta_\infty$-(Young), determined from the surface tensions and using Young's equation. For the medium and weak attraction, $f \times \rho_w = 0.6$ and $\times \rho_w = 0.3$, there is a fair agreement between the angles obtained from Young's equation and the angles determined from the profiles of the liquids at the wall; but for the strong surface attraction, Young's equation predicts an angle near wetting, whereas both the droplets and the liquid within the walls have contact angles that are significantly larger.

The droplets are often assumed to be spherical segments; this is, however, not correct as can be seen in Figures 3 and 6. Figure 6 shows the profiles of the four droplets at the weak attractive surface with $f \times \rho_w = 0.3$. The figure illustrates that for this attraction there is a monotonic variation in the surface of the droplets down to the point of contact and that the contact angle is indeed established within the first two fluid layers of particles in the droplets.

As discussed in the Introduction, the deviation from Young's equation is often treated using eq 4 with a correction for line tension and quite often with the result that one obtains a negative "line tension", $\tau$. We also obtain (Tables 2−4) a weak but significant increase in the contact angle with droplet size corresponding to a negative line tension. As pointed out in the Introduction, this size effect could be caused by several factors.

## IV. Discussion

The present simulations demonstrate that it is possible to determine the contact angle with particle-size resolution at the (perfect planar) solid surface and that this nanoscale contact angle is a limit value of a monotonic varying density profile (Figure 6). Although the $u_{9-3}(z)$ potential has been used successfully in many investigations of wetting and pre-wetting, it is, however, a simplification of the real force-field at a planar solid surface, and the nanoscale-contact angle might be affected by the particle structure of the solid surface. A heterogeneous solid substrate is known, from both experiments and calculations[20] to affect the contact of the liquid droplet, and the effect is described by Wenzel's law[21] or Cassie's law.[22]

Young's equation, as well as its extension (eq 4) is used extensively for determination of solid−liquid free energies and for droplet and interface analysis. The equation is correct in the thermodynamic limit of macroscopic droplets with bulk liquid property and for models with nearest-neighbor interactions,[23] where the range of (solid) attraction does not exceed the thickness of the interfaces. For real systems and smaller droplets with the surface forces acting over longer ranges, the free energy-density in the contact zone can not, in a well-defined way, be separated into three subcontributions for unperturbed interfaces. Nevertheless, Young's equation could still be valid. We obtain agreement within the accuracy of the computations for two of the three values of the strength of attractions, $f \times \rho_w = 0.3$ and $f \times \rho_w = 0.6$, respectively; but for $f \times \rho_w = 1$ the

observed angles, $\theta$ and $\theta_\infty$, deviate from Young's contact angle, $\theta_\infty$(Young) (Table 4). Young's equation predicts an angle of 6°, that is, an angle near wetting, whereas the obtained angles from droplets and a liquid at a planar wall are in the range of 35−45°.

The Lennard-Jones dispersion force-field is common for all matter, and although this pairwise additive force is weak, the net-contribution from a semi-infinite solid declines as $z^{-3}$ with respect to the distance, $z$ from the solid surface and results in a nonuniform zone of many particle diameters. This net force affects the shape of droplets and their contact angles. In systems with stronger and more long-ranged attractive forces, the resulting nonuniform contact zone is even larger. This fact implies that self-assembly phenomena on attractive surfaces with small contact angles on nanoscale levels might not be described appropriately by Young's equation and its extension for curvature and line tension.

## References and Notes


(1) Young, T. *Philos. Trans.* **1805**, *95*, 84.
(2) Saville, S. *J. Chem. Soc., Faraday Trans.* 2 **1977**, *73*, 1122.
(3) Werder, T.; Walther, J. H.; Jaffe, R. L.; Halicioglu, T.; Koumoutsakos, P. *J. Phys. B* **2003**, *107*, 1345.
(4) Hong-Kai, G.; Hai-Ping, F. *Chin. Phys. Lett.* **2004**, *22*, 787.
(5) Li, D. *Colloids Surf., A* **1996**, *116*, 1.
(6) Pompe, T.; Herminghaus, S. *Phys. Rev. Lett.* **2000**, *85*, 1930.
(7) Checco, A.; Guenoun, P. *Phys. Rev. Lett.* **2003**, *91*, 186101.
(8) Boruvka, L.; Neumann, A. W. *J. Chem. Phys.* **1977**, *66*, 5464.
(9) The derivation of the "Tolman correction" to the surface tension for curvature is given in the following: Rowlinson, J. S.; Widom, B. *Molecular Theory of Capillarity*; Oxford University, New York, 1963; p 031601.
(10) For MD details, see Toxvaerd, S. *Mol. Phys.* **1991**, *72*, 159. Temperature is in units of $\epsilon/k$, length is in units of $\sigma$, and time is in units of $\sigma\sqrt{(m/\epsilon)}$ where $m$ is the mass of a particle. The time step is 0.005. ($N$, $V$, $T$) simulations are performed using a Nosé-Hoover thermostat.
(11) Ebner, C.; Saam, W. F. *Phys. Rev. Lett.* **1977**, *38*, 1486.
(12) Fan., Y.; Monson, P. A. *J. Chem. Phys.* **2002**, *117*, 10303.
(13) Toxvaerd, S. *J. Chem. Phys.* **1993**, *99*, 6897.
(14) Buff, F. P. Z. *Elektrochem.* **1952**, *56*, 311.
(15) Toxvaerd, S. *J. Chem. Phys.* **1981**, *74*, 1998.
(16) Chapela, G. A.; Saville,G.; Thomson, S. M.; Rowlinson, J. S. *J. Chem. Soc., Faraday Trans. 2* **1977**, *77*, 1133.
(17) Barker, J. A. *Mol. Phys.* **1993**, *80*, 815.
(18) Stillinger, F. H. *J. Chem. Phys.* **1963**, *38*, 1486.
(19) An error function describes the liquid−gas density profiles marginally better, but usually one uses a tanh function. For details see, e.g., Toxvaerd, S.; Stecki, J. *J. Chem. Phys.* **2001**, *115*, 1928.
(20) De Coninck, J.; Ruiz, J.; Miracle-Solé, S. *Phys. Rev. E* **2002**, *65*, 036139.
(21) Wenzel, R. N. *Ind. Eng. Chem.* **1936**, *28*, 988.
(22) Cassie, A. B. D. *Discuss. Faraday Soc.* **1952**, *57*, 5041.
(23) de Coninck, J.; Dunlop, F. *J. Stat. Phys.* **1987**, *47*, 827.